Supporting information for: "Spin-component scaled and dispersion corrected second-order Møller-Plesset perturbation theory: A path toward chemical accuracy"

Chandler Greenwell,[†] Jan Řezáč,[‡] and Gregory J. O. Beran[*,†]

[†]*Department of Chemistry, University of California, Riverside, California 92521 USA*

[‡]*Institute of Organic Chemistry and Biochemistry, Czech Academy of Sciences, 166 10 Prague, Czech Republic*

E-mail: gregory.beran@ucr.edu

Contents

The SI provides additional insight on (1) an alternative parameter search where a Bayesian search algorithm with Gaussian processes was explored, (2) how the damping function changes from MP2D to SCS-MP2D, (3) a table displaying the percent relative root mean square errors for each method on each benchmark data set, and (4) the full anthracene photodimer potential energy curve.

S1 Bayesian Parameter Search Algorithm

Bayesian optimization is intended to find optimal parameters (x_1, ..., x_n) for an unknown function f(x_1, ... x_n). For example, Bayesian optimization is useful for finding optimal hyperparameters in machine learning models, especially when the model is expensive to train. If analytic gradients of the objective function are available, then Bayesian optimization will likely be less efficient than a gradient-based optimizer. For that reason, the evolutionary algorithm with gradient-based minimization was employed for the primary parameter search in this work. However, given the rough SCS-MP2D parameter landscape with many local minima, Bayesian optimization was employed as a secondary check for discovering any potential alternate parameter sets that might have been missed in the evolutionary search.

A Bayesian algorithm with Gaussian processes was used in this work as a probe of the likely parameter space, and as a convergence test for the genetic/gradient optimization algorithm. The Bayesian optimizer was seeded with top performing parameter sets from the evolutionary algorithm/gradient-based optimizations. The progression of the optimizer is shown in Figure S1. Initially the Bayesian algorithm probes the potential energy landscape of the optimization problem with the seed points, then a predefined number of random points are sampled and used to construct a probability model of the objective function for the parameter space. After the random points are sampled, the most promising points according to the probability model are sampled. The probability model is continuously updated as new points are sampled. As exemplified by Figure S2, none of the Bayesian search runs identified any parameter sets that were better than what the evolutionary algorithm searches found. This result increases the confidence that an optimal or near-optimal set of parameters was discovered for the chosen training data.

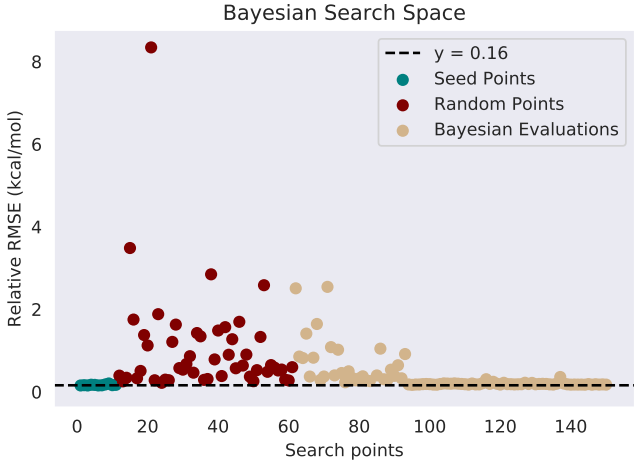

Figure S1: Example of a Bayesian parameters search: (1) the optimizer is seeded with good parameter sets from the genetic/gradient optimizer, (2) 50 random points are sampled within a predefined sample space, and (3) new points are sampled based on a function constructed from the seeded and random guess points.

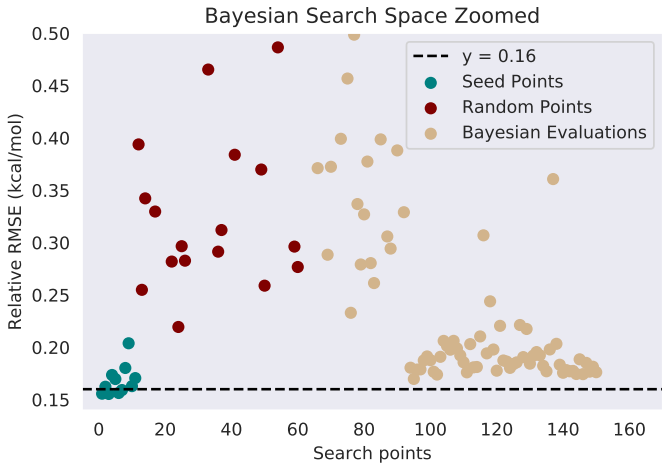

Figure S2: Zooming in on the search space shows how the Bayesian optimizer finds new parameter sets that perform well, but do not match the performance of the best parameter sets from the genetic/gradient optimizer.

S2 Comparing the Tang-Toennies damping function in MP2D and SCS-MP2D

Here, the Tang-Toennies damping function is plotted as a function of the interatomic distance between three different atom pairs (C-C, C-H, and H-H) for our original MP2D method and SCS-MP2D. Compared to MP2D, SCS-MP2D allows the dispersion term to contribute more at shorter ranges. It is possible that this is in response to the reduced scaling of the opposite-spin C_{os} and same-spin C_{ss} coefficients in SCS-MP2D. Their respective values of 0.8263 and 0.9004 are both less than 1. Unlike the original SCS-MP2 and SCS-MI-MP2 methods, SCS-MP2D has both spin components reduced from the canonical value of 1. It is also worth observing that the C_{os} and C_{ss} values are very similar. This suggests it could be possible to develop an SCS-MP2D type method with a single scaling coefficient for the MP2 correlation energy.

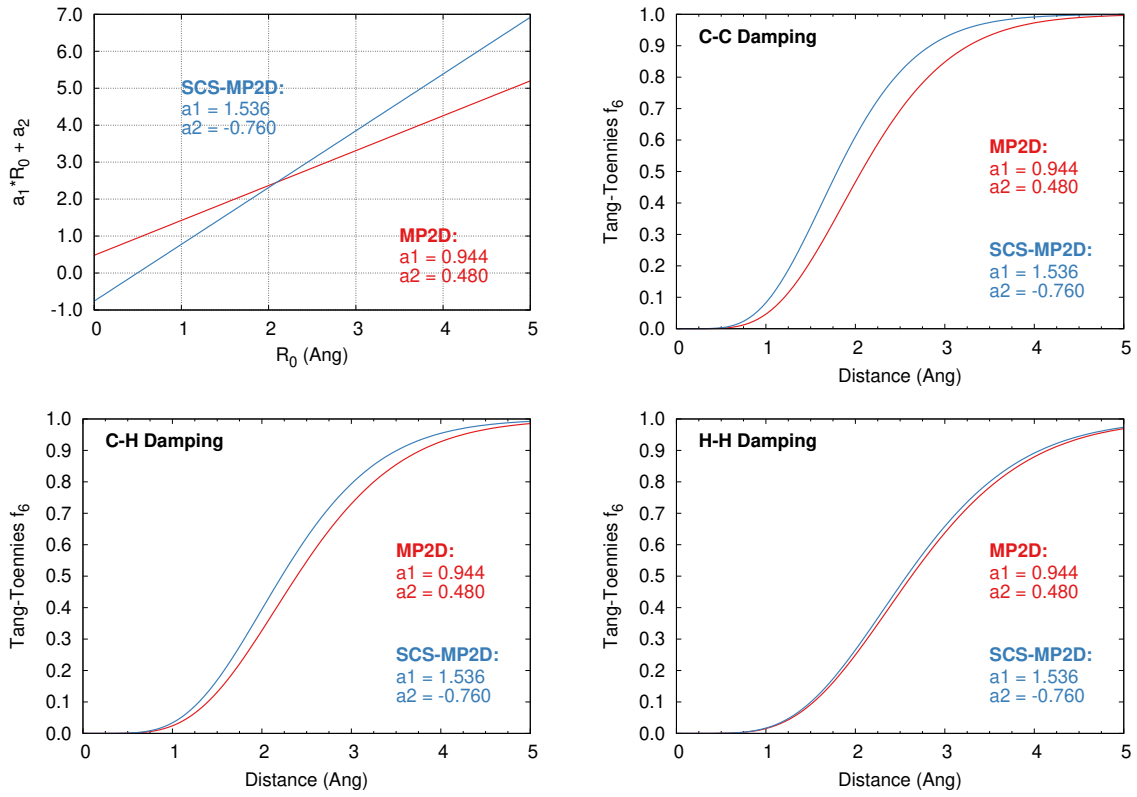

Figure S3: Examination of the Tang-Toennies damping function f_6 as a function of the interatomic distance, R, for three atom-type interactions.

S3 Percent Weighted Root Mean Square Errors for Benchmark Data Sets

As a companion to Table 2 in the main paper, Table S1 summarizes the relative root-mean-square errors for the data sets

Table S1: Relative root mean square error (%) calculated by dividing the RMSE by the mean absolute value of the reference energies and multiplying by 100. The asterisk (⋆) indicates data sets that were used to fit SCS-MP2D.

Data Set	MP2 CBS	MP2D CBS	SCS-MP2D CBS	DSD-BLYP-D3(BJ) def2-QZVP	revDSD-PBEP86-D3(BJ) def2-QZVP	ωB97X-V def2-QZVP	ωB97M-V aQZ
Intermolecular Interactions							
S66x8	16.71	3.92	3.10⋆	4.51	4.08	5.32	2.73
3B-69 Dimers	8.08	5.08	4.35	4.70	4.57	4.85	4.07
SSI	4.31	1.87	2.02	1.80	1.45	2.40	1.80
HBC6	2.96	2.46	2.36	3.44	1.58	2.98	2.20
NBC10	98.56	18.62	8.71	20.97	4.43	21.87	10.60
Charge Transfer	19.61	4.06	2.46	5.52	4.48	4.12	3.26
HB375	7.69	2.86	2.26	2.50	2.37	3.09	3.38
IHB100	2.36	2.44	1.77	2.19	1.38	1.93	1.88
Conformational Energies							
SCONF	6.72	7.65	3.98⋆	5.74	2.93	4.57	5.15
ACONF	6.00	3.60	6.32	4.53	12.84	3.27	4.53
Amino20x4	10.66	6.89	7.30	6.66	6.82	9.86	9.84
MCONF	20.52	8.13	6.62	11.15	3.92	5.43	7.93
PCONF21	68.45	25.90	19.36	29.39	14.02	21.58	42.81
Reaction Energies							
DARC	12.22	5.84	4.35⋆	3.37	1.96	13.49	3.01
ISO34	11.53	9.76	6.62	7.26	3.34	10.68	5.66
ISOL24	16.74	12.64	10.07	12.19	7.79	18.92	10.87
IDISP	49.40	9.97	9.06	11.27	4.70	27.28	19.87

S4 Full Anthracene Photodimerization Potential Energy Curve

This plot shows the full potential energy curve for the anthracene photodimerization. As stated in the main paper, the restricted, single-reference electronic structure models are probably not reliable in the intermediate regime between the two wells due to the substantial static correlation associated with forming/breaking two C-C single bonds.

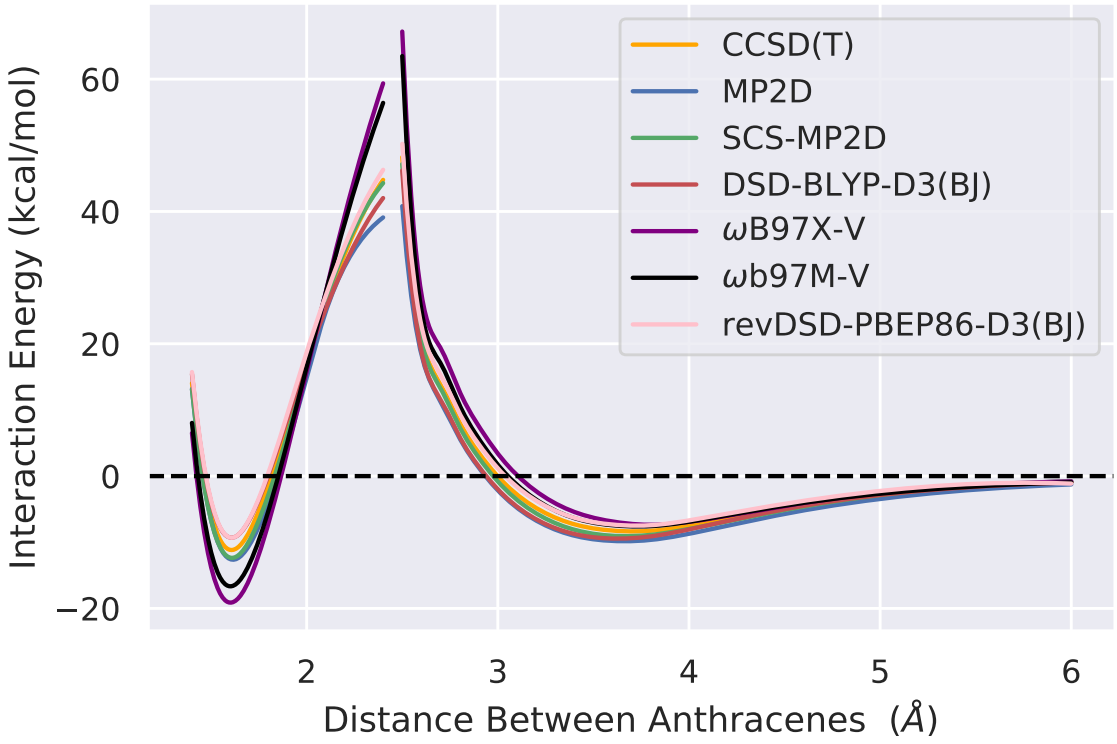

Figure S4: 1-D potential energy scan following the dissociation of an anthracene photodimer to a separated π-stacked dimer